Study of Varying Weight%, Particle Size and Artificial Aging of Al_2O_3 on the Hardness and Wear Resistance of Al 6082 Alloy Composites by Stir Casting

N. Sirajudeen, R. Karunanithi, and M. Abdur Rahman

Abstract In this study, the effect of artificial aging, particle size, different weight fractions (1, 1.5, 2, and 2.5%) of Al_2O_3 on the hardness and wear resistance of Al 6082 alloy composite produced by stir casting method is studied. Al 6082 alloy composite specimens strengthened individually with Al_2O_3 particles of 45 μm and 40–50 nm were produced by stir casting method. The composite specimens were first solutionized followed by artificial aging at 180 °C for various time periods (1, 2, 4, 6, 8, 10, 12, 14, 16, 18 and 20 h). The hardness and wear tests were performed on the heat-treated and non-heat-treated specimens. Vickers microhardness tests demonstrated a tremendous improvement in the composites' VHN values due to artificial aging and the addition of varying wt% of micron/nano-sized Al_2O_3 reinforcement. The T6-treated Al 6082 alloy composite specimens reinforced with nano-Al_2O_3 particles showed an enhancement in VHN microhardness and wear resistance when compared to the pure Al 6082 alloy and composite specimens reinforced with micron-sized Al_2O_3 reinforcement. Pin-on-disc wear testing demonstrated that T6 specimens reinforced with nano-Al_2O_3 exhibited enhanced wear resistance than the composite specimens reinforced with micron-sized ceramic reinforcement. Worn surface morphology was carried out using FESEM to study the mode of wear.

Keywords Stir casting · Nano alumina · Al metal matrix composite · Aging · Wear

1 Introduction

Aluminium matrix composites (AMCs) are widely used for the manufacture of automobile, aerospace, marine and military components due to their excellent mechanical, tribological and corrosion properties. Investigations are going on in a large scale all over the world to enhance its properties by using innovative production methods and also by the inclusion of reinforcements [1–3]. The addition of certain particulates to the base metal matrix enhances its properties in terms of increase in strength,

N. Sirajudeen · R. Karunanithi (✉) · M. Abdur Rahman
Department of Mechanical Engineering, B.S.A.R Crescent Institute of Science and Technology, Chennai 600048, India
e-mail: karunanithi@crescent.education

L. Ganippa et al. (eds.), *Advances in Design and Thermal Systems*, Lecture Notes in Mechanical Engineering, https://doi.org/10.1007/978-981-33-6428-8_14

hardness, wear, thermal and corrosion resistance. Thus, the particulate-reinforced aluminium matrix composites (PRMMC) are rapidly replacing the conventional aluminium matrix composites owing to their superior performance. A lot of research work is going on to produce them with enhanced properties, especially for aerospace, structural and military applications [4–7]. The addition of strengthening media to the base aluminium matrix causes many beneficial changes like grain refinement, enhanced dislocation density and the ability of the base matrix to transfer the applied load to the ceramic reinforcement thereby increasing its strength [8, 9]. Among aluminium alloys, the age hardenable, Al–Mg–Si alloy commonly referred as 6XXX series alloys are widely used for structural applications possess a lower density, good strength, exceptional formability, and good corrosion resistance [10–12]. PRMMCs are fabricated by many techniques like liquid metal infiltration, mechanical alloying, squeeze casting, friction stir processing, etc. and among them, the stir casting technique has proven to be a highly economical route. Recent studies have revealed the possibility of attaining a good homogenous dispersion of the reinforcement particles in the base alloy matrix by optimizing the stir casting process parameters like stirring speed, pouring time, controlled atmosphere, the temperature of the liquid metal, preheating of the mould, etc. [13, 14].

The fabrication of composite involves melting of the metal, addition of ceramic particulates and mechanically mixing them uniformly in the molten matrix using a stirrer setup [15]. The commonly used ceramic reinforcements for enhancing the mechanical, tribological and corrosion behaviour of the metal matrix composites are SiC, boron carbide, Al_2O_3 and zirconia [16–21].

Among them the Al_2O_3 particles are widely used as reinforcement material owing to its exceptional mechanical, wear and corrosion properties [22]. Among the 6XXX series age hardenable alloys, the Al 6082 alloy with outstanding mechanical properties occupies a significant place for lightweight applications [23]. GP zones develop due to nucleation of precipitates during solution treatment of age hardenable alloys [24].

Previous research studies on age-hardenable alloys have indicated the development of (intermetallic) phases [25]. Although the effect of varying particulate size and weight fraction of ceramic reinforcement has been studied previously, very less research has been done on the effect of heat treatment and varying particle of Al_2O_3 on the hardness and wear behaviour of the Al 6082 alloy composite. Thus, the novelty of the present investigation is to study the combined influence of artificial aging (1, 2, 4, 6, 8, 10, 12, 14, 16, 18 and 20 h) and varying particle/weight% of Al_2O_3 particles on the hardness and wear resistance of Al 6082 alloy composite by stir casting route. The other novelty of this research is apart from comparing the effect of T6 aging; it studies the effect of T7 or overaging (heat treatment) on the hardness of Al 6082 alloy composite specimens reinforced separately with coarse and nano-Al_2O_3 reinforcement particles. The wear resistance of the test specimens is studied using a pin-on-disc wear tester under varying load conditions.

2 Materials and Methods

2.1 Sample Preparation

The commercially available Al 6082-T6 alloy and Al_2O_3 powder of 45 μm size was chosen as the matrix and reinforcement material, respectively. Toluene was added to avoid a rise in temperature and clustering. The particle size analysis (Zeta Nano ZS, Malvern, UK) showed that the final particle size after ball milling of micro-sized Al_2O_3 was 40–50 nm. Preheated (250 °C), Al_2O_3 reinforcement particles with varying weight % (1, 1.5, 2, and 2.5%) and size (45 μm/ 40–50 nm) were added individually to the base matrix to get two sets of cast specimens, i.e., one set of samples was reinforced with coarse alumina and the next set of samples with nano-alumina. Stirring time and speed were fixed as 10mins and 300 RPM, respectively, to obtain a vortex. Stirring temperature was maintained between 830 and 850 °C. Hexachloroethane (C2Cl6) tablets were used to get rid of the trapped gases.

Later the two different sets of Al 6082 alloy composite reinforced separately with varying weight fraction of coarse and nano-Al_2O_3 particles were poured into a preheated die, of 20 mm diameter and 200 mm height. After the solidification process, the cast samples were ejected from the die and machined to ASTM standard dimensions for hardness and wear tests.

2.2 Aging

The specimens were initially solutionized at 480 °C for a period of 1 h in an induction furnace. The solutionized specimens were quenched followed by artificial aging for various time periods of 1, 2, 4, 6, 8, 10, 12, 14, 16, 18 and 20 h at 180 °C.

2.3 Hardness Measurement

VHN measurement was performed on a Vickers microhardness testing machine with a load capacity of 50 kgf and a ball indenter diameter of 5 mm. The test was repeated at five different locations for reproducibility, and the average values were tabulated.

2.4 Wear Test

Wear test of the composite was analysed under varying load (15 N, 20 N, 25 N and 30 N) conditions. Machining was performed on the stir cast specimens such that it had a diameter and a height of 6 mm and 15 mm, respectively. Volumetric wear rate of

the specimens was performed on a pin-on-disc wear testing machine (Model: TR20-LE) with a sliding speed of 2 ms^{-1} against EN32 steel disc (500HV) of 100 mm track diameter. Acetone was used as a cleaning substance for the specimens.

2.5 XRD and FESEM

The cast composite specimens were mechanically polished using 800, 1000, 1200, 1500 gr SiC emery sheets. The polished samples were cleaned with distilled water and acetone, further cloth polishing of the specimens was performed by applying a diamond paste (0.5 μm). The specimens were later etched using Keller's reagent, before conducting the FESEM (Model: SUPRA 55-CARL ZEISS, GERMANY) and XRD analysis (PANalytical X-ray diffractometer).

3 Results and Discussion

3.1 Vickers Microhardness

Vickers microhardness testing machine was used for hardness test for both the non-aged and aged specimens of Al 6082 alloy composites. The VHN plot shown in Figs. 1 and 2 shows that the microhardness of Al 6082 alloy composite increases due to the addition of both coarse or nano-Al_2O_3 reinforcement. Nevertheless, the nano-Al_2O_3-reinforced specimens out performed its coarse Al_2O_3-reinforced counterpart. The specimens reinforced with 2.5 wt.% of nano Al_2O_3 reinforcement attained a maximum VHN of 238, i.e., peak aged hardness was attained after 6 h of aging. This can be ascribed to precipitation hardening as well as the hard nature of the nano sized Al_2O_3 particulates, which acted as barriers to dislocation motion resisting the loads related to indentation during VHN tests [26, 27].

Based on the VHN microhardness results, the aged samples can be categorized into underaged, peak aged and overaged samples. The increase or decrease in the hardness of the specimens can be related to the kinetics of aging which affects the shape, size and dispersion of precipitates in the base alloy matrix [28].

The graphs in Figs. 1 and 2 indicate an enhancement of VHN microhardness values due to the addition of both coarse and nano-sized reinforcement; however, it is worth noting that the aged specimens outperformed the non-aged samples. The other reason for the improvement of VHN can be attributed to the addition of nano-sized reinforcement particles [29].

With an increase in the weight fraction of alumina particles of nano-size, a higher dislocation density existed due to the thermal mismatch between the nano Al_2O_3 and the base Al 6082 alloy matrix. This increased dislocation density in the base matrix increased the hardness of the composite [30].

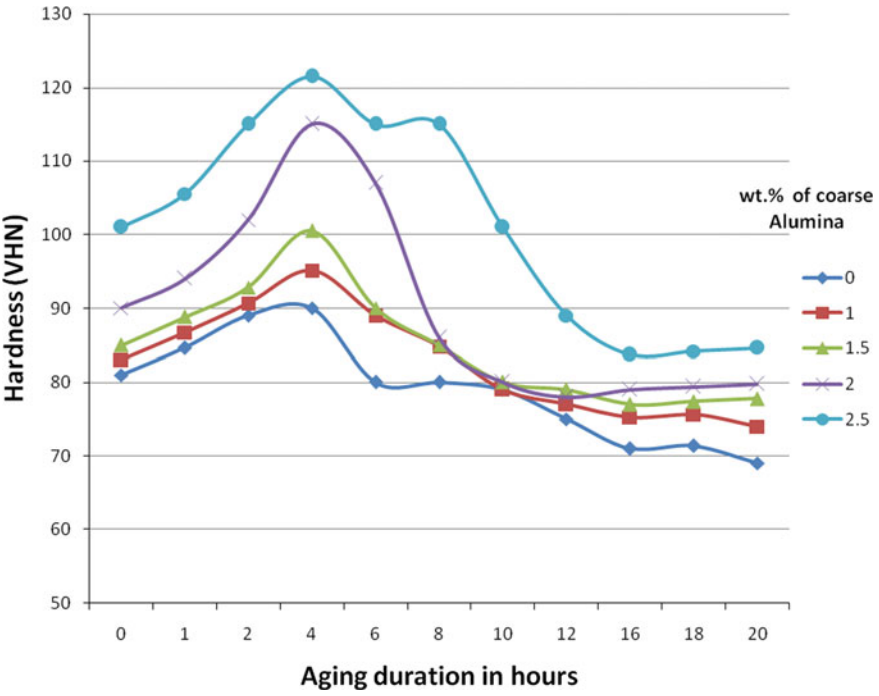

Fig. 1 VHN versus aging duration plot of the Al 6082 alloy composite reinforced with coarse Al_2O_3 particles

It is clear from Figs. 1 and 2 that artificial aging of both the unreinforced Al 6082 alloy and its reinforced composite specimens led to an increase in the VHN microhardness. The graphs indicate a sharp increase in the VHN microhardness immediately after the solution treatment followed by artificial aging. The coarse Al_2O_3-reinforced composite specimens (refer Fig. 1) show a tremendous increase in VHN microhardness up to 122 VHN (peak aged hardness) after 4 h of aging beyond which the specimens showed a gradual beg off in its VHN value. The peak aged (T6) hardness values of composite specimens reinforced with 1, 1.5, 2, 2.5% of coarse Al_2O_3 particles are 90, 95, 101, 115 and 122 VHN, respectively. Overaging (T7) occured in the range of 18–20 h when the samples reinforced with different wt.% of coarse Al_2O_3 particles attained their lowest hardness.

Figure 2 shows the VHN values of aged specimens reinforced with 1, 1.5, 2 and 2.5% of nano Al_2O_3 particles as 119, 141, 143, 200 and 238 VHN, respectively, after 6 h of aging. Similarly overaging (T7) occurred in the range of 18–20 h during which the samples reinforced with nano-Al_2O_3 particles reached their lowest microhardness values. Nevertheless, the nano-Al_2O_3-reinforced samples outperformed the coarse Al_2O_3-reinforced samples even at overaging (T7) conditions in terms of microhardness values. Thus, the VHN microhardness results reveal that the nano-Al_2O_3-reinforced Al 6082 alloy composite samples bettered the coarse Al_2O_3 reinforced

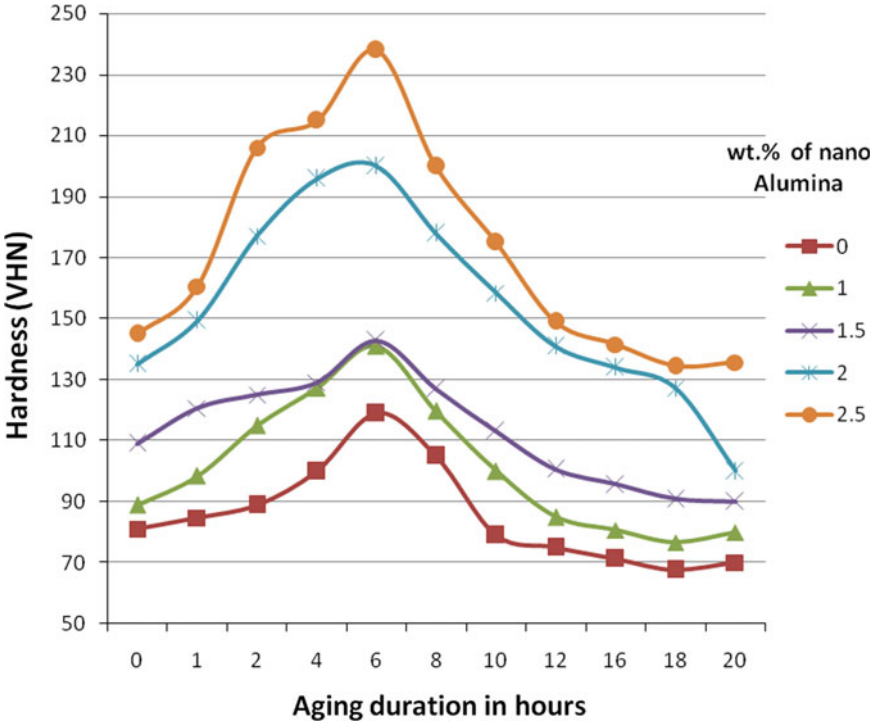

Fig. 2 VHN versus aging duration plot of the Al 6082 alloy composite reinforced with nano-Al_2O_3 particles

Al 6082 alloy composite specimens. Usually, grain boundary acts as the preferential place for the nucleation of precipitate phases. During heat treatment, the diffusion of Mg and Si is quite significant for the formation of Mg_2Si precipitates. After the attainment of a supersaturated solid solution, artificial aging is performed by heating the specimens at a suitable temperature of 180 °C, which will speed up the process of Mg and Si diffusion, leading to the formation of (stable) Mg_2Si precipitate [31]. It has been reported that the decomposition of supersaturated solid solution occurs as a result of aging. Hence, with aging rate is proportional to the degree of supersaturation [32]. During age hardening, the rearrangement of atoms within the crystal lattice occurs. Next forms the clusters and GP zones. In this stage, mechanical properties are improved due to the occurrence of microstrains in the crystal lattice. When compared to the pure alloy, the composite specimens undergo accelerated aging due to the occurrence of a large dislocation density near the Al 6082 matrix—Al_2O_3 interface [33]. Previous studies on the Al 6XXX alloys show the following sequence of aging: [31, 34].

Initially, the supersaturated solid solution transforms into cluster of solute atoms followed by primitive Guinier–Preston zones which transform into needle-shaped GP zones which are rod-shaped, metastable, hexagonal and semi-coherent-β phase.

The formation of GP zones is a complex process which involves the formation of clusters of vacancies and silicon atoms followed by the precipitation of Mg atoms on nuclei [35]. Then forms the stable, incoherent, cubic, Mg_2Si precipitate (β phase). It has also been reported that the solutionizing temperature plays a crucial role in increasing the strength of the Al 6061 Al/SiC composite. The report also suggests a correlation between the hardness and the aging temperature/duration owing to the phase transformations occurring during heat treatment [34].

XRD graphs of both the T6-aged Al 6082 alloy (refer Fig. 3) and the T6-aged Al 6082 alloy composite reinforced with 2.5 wt% of nano Al_2O_3(refer Fig. 4) reveal the formation of the stable Mg_2Si precipitates on account of the precipitation hardening phenomenon.

The enhanced VHN microhardness of the Al 6082 alloy composite compared to the unreinforced alloy could be attributed to its better aging kinetics behaviour. The acceleration of aging occurs due to a high concentration of dislocations near the vicinity of the alloy matrix–ceramic reinforcement interface [36]. The presence of high density of dislocations paved the way for the occurrence of heterogeneous nucleation sites which are precursors for the formation of precipitates and enhances higher diffusivity of alloying elements [34–36].

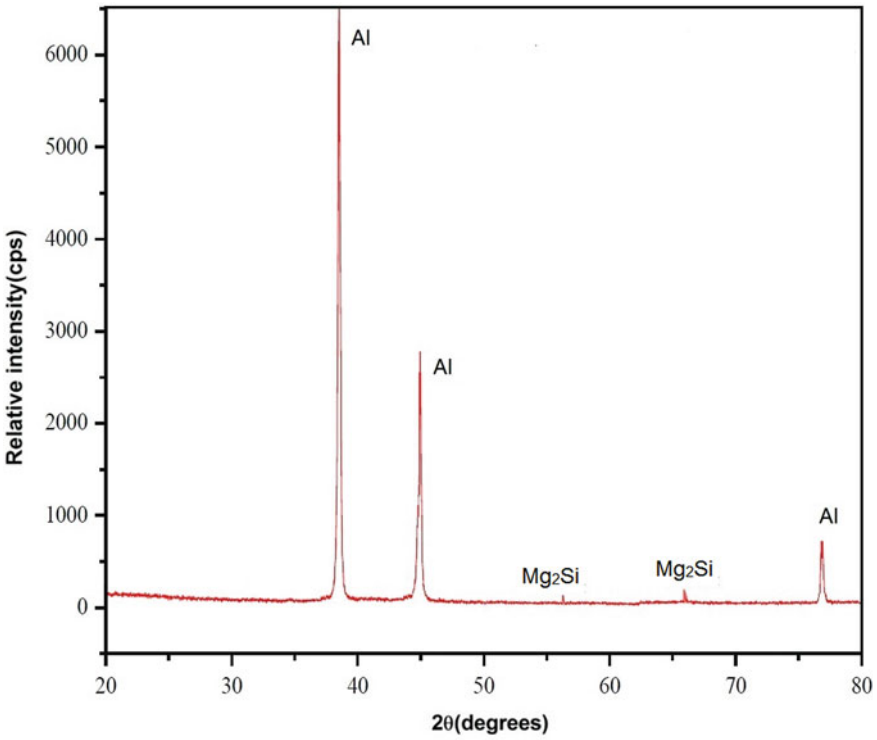

Fig. 3 XRD plot of Al 6082 alloy subjected to T6 aging

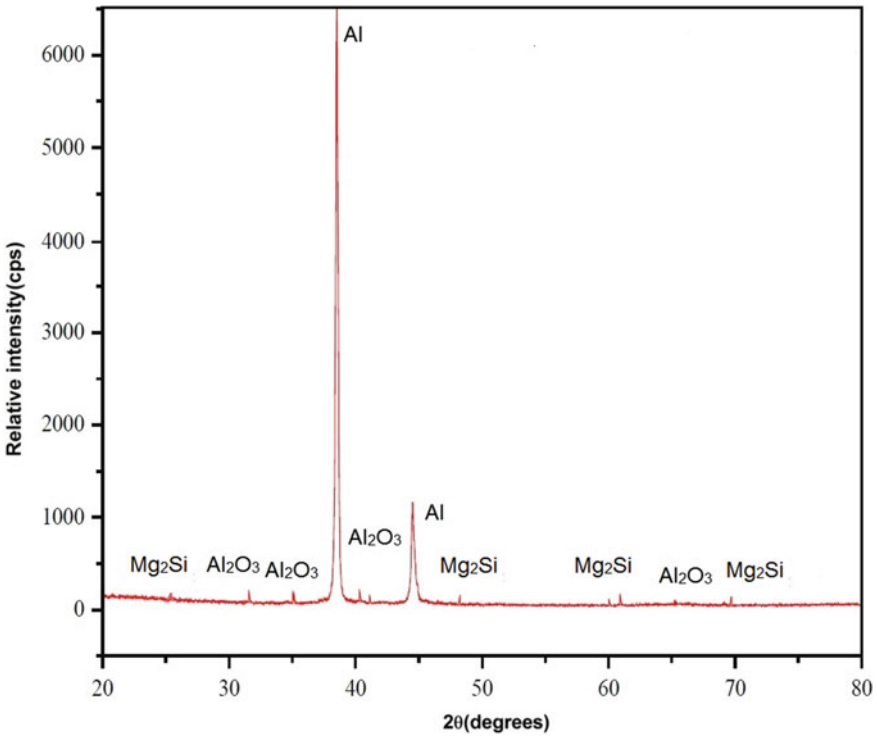

Fig. 4 XRD plot of Al 6082 alloy reinforced with 2.5 wt% of nano Al_2O_3 subjected to T6 aging

3.2 Wear Test

Wear tests were performed on both the non-aged and T6-aged samples with and without reinforcement (micro/nano). Figures 5, 6, 7, 8, 9, 10, 11 and 12 demonstrate an enhancement of wear resistance of the test specimens due to the addition of varying weight fraction and particle size of the reinforcement. With the increase in the applied

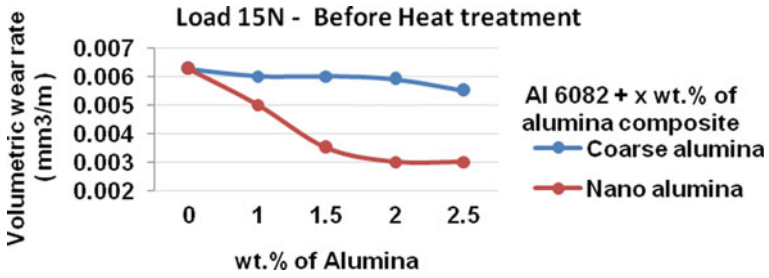

Fig. 5 Wear rate of Al 6082 alloy composite at load of 15 N, before heat treatment

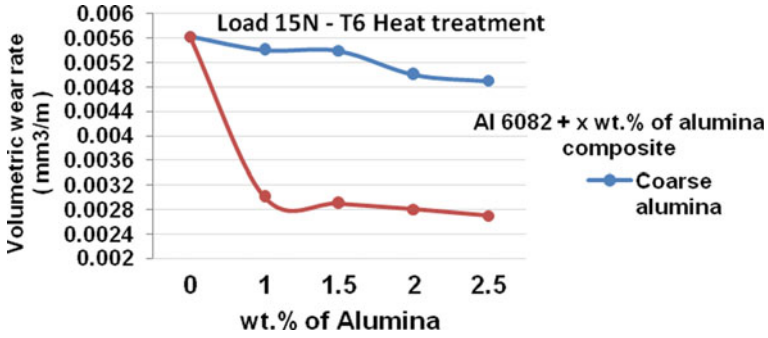

Fig. 6 Wear rate of Al 6082 alloy composite at load of 15 N, after T6 aging treatment

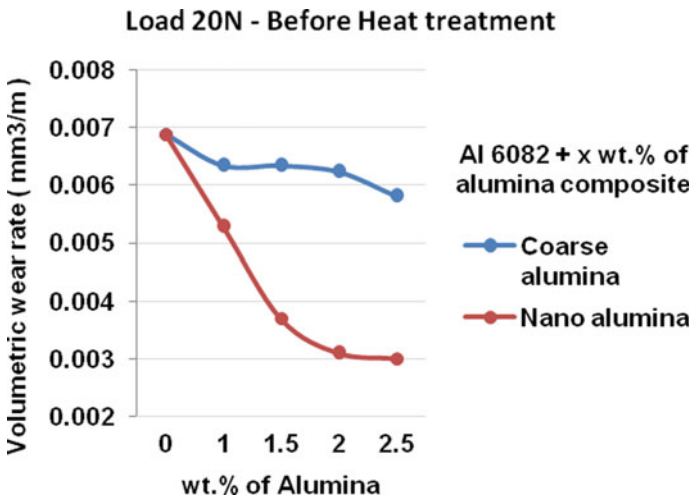

Fig. 7 Wear rate of Al 6082 alloy composite at load of 20 N, before heat treatment

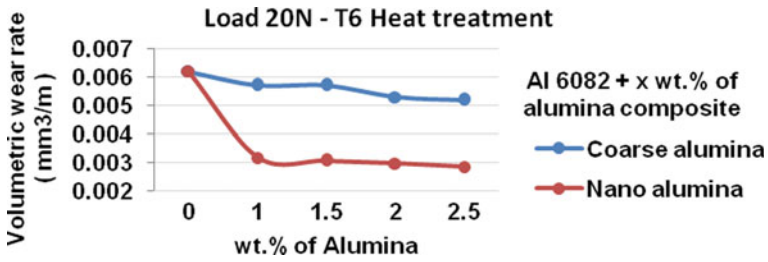

Fig. 8 Wear rate of Al 6082 alloy composite at load of 20 N, after T6 aging treatment

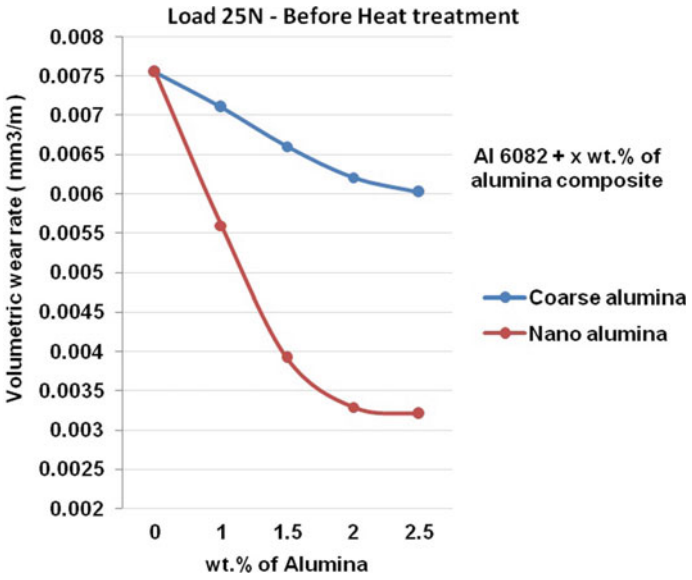

Fig. 9 Wear rate of Al 6082 alloy composite at load of 25 N, before heat treatment

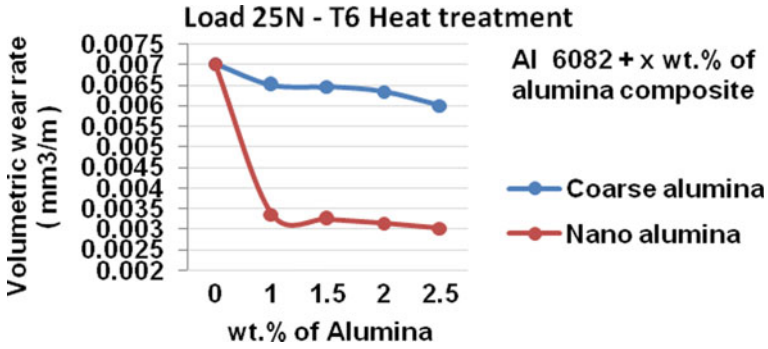

Fig. 10 Wear rate of Al 6082 alloy composite at load of 25 N after T6 aging treatment

load, the rate of volumetric wear also increases. Nevertheless, the volumetric wear rate of the pure alloy and the coarse Al_2O_3-reinforced samples were higher than that of the nano-Al_2O_3-reinforced Al 6082 alloy composite specimens indicating enhanced resistance to wear due to the addition of nano-Al_2O_3 particles. The wear graphs also show that the T6-aged specimens reinforced with nano-Al_2O_3 particles outperformed the other sets of specimens, i.e., unreinforced Al 6082 alloy and the coarse Al_2O_3-reinforced Al 6082 alloy composite (under both aged and non-aged conditions) showing an enhanced wear behaviour. Thus, the pin-on-disc wear testing results (refer Figs. 6, 8, 10 and 12) showed that the T6-aged, nano-Al_2O_3-reinforced

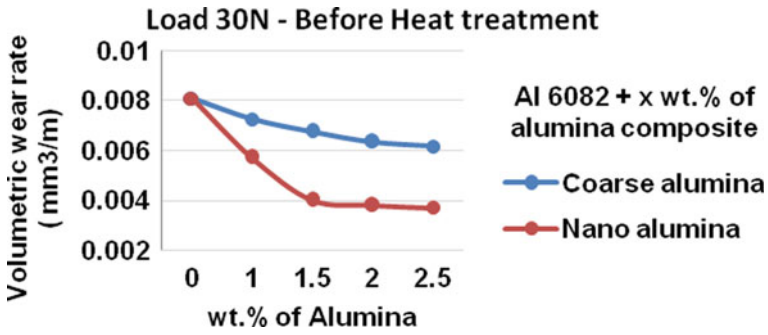

Fig. 11 Wear rate of Al 6082 alloy composite at load of 30 N before heat treatment

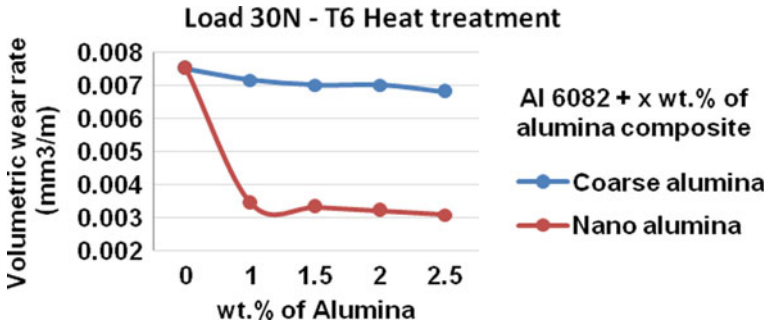

Fig. 12 Wear rate of Al 6082 alloy composite at load of 30 N after T6 aging treatment

Al 6082 alloy composite specimens demonstrated an enhanced wear resistance under varying applied loads of 15, 20, 25 and 30 N.

SEM micrographs of the worn samples of T6-aged and non-aged composite specimens as well as the unreinforced specimens are shown in Figs. 13, 14, 15, 16, 17, 18 and 19. SEM images clearly indicate that the non-aged Al 6082 alloy and its composites have suffered more damage compared to the aged specimens. Development of microcracks as indicated in Figs. 15, 17 and 19 could be ascribed to the occurrence of fatigue wear due to repeated loading during wear test runs. Figure 16 shows the formation of deep grooves of various sizes which lead to subsurface crack propagation along the direction of sliding. With the increase in the applied load, delamination mode of wear occurs (refer Fig. 18). The pure Al 6082 alloy's worn surface (refer Fig. 13) is characterized by large craters, indicating that the specimen has undergone severe plastic deformation due to its inability to resist the repeated loads during sliding test runs. The size of cracks and grooves of the pure Al 6082 alloy indicates the occurrence of abrasive mode of wear due to severe plastic deformation. The peeling away of the outer layer which is occupied by the hard nano-Al_2O_3 particles also indicates that the mechanism of wear is abrasive in nature (refer Figs. 13 and 14).The severe damage could also be attributed to the direct contact between the metal to

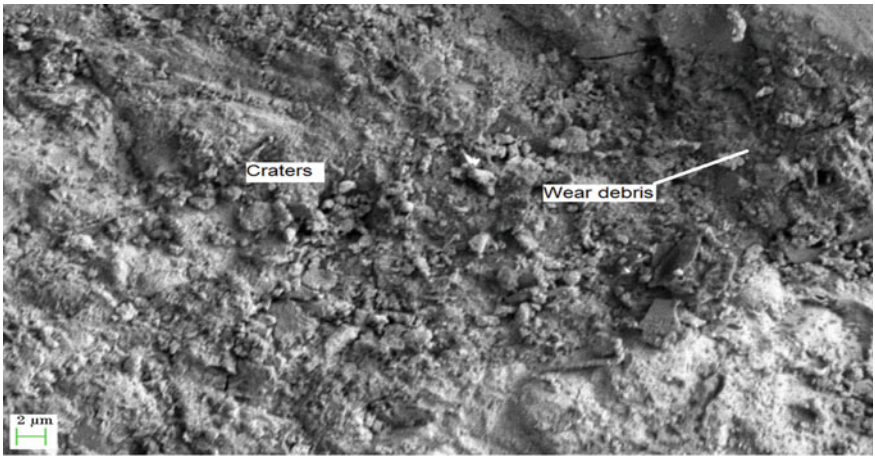

Fig. 13 SEM micrograph of (non-aged) unreinforced Al 6082 alloy revealing craters and the accumulation of wear debris

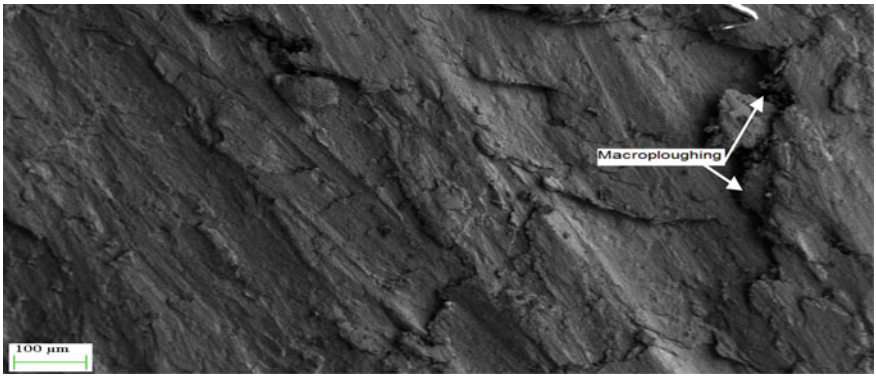

Fig. 14 SEM micrograph of (non-aged) unreinforced Al 6082 alloy revealing severe damage due to macroploughing

metal interface between the matrix and the counter steel disc. The increase in the applied load softens the base matrix leading to more material loss. The worn surface of the reinforced specimens is characterized by particle pull out associated with fine to distinctive groove formations (refer Fig. 15). With the increase in the applied load, the protrusion of ceramic particles from the worn surface leads to abrasive type of wear. This could be ascribed to the high plastic strain which destabilizes the ceramic particle from the worn surface. During sliding wear, the loosening of the ceramic particles takes place which later get confined between the faying surfaces. A mechanism known as three-body abrasion occurs. The tribo-film comprises of confined Al_2O_3 particles and wear debris emerging between the faying surfaces of Al 6082 alloy matrix and the counter steel disc surface. This wear-resistant film decreases the

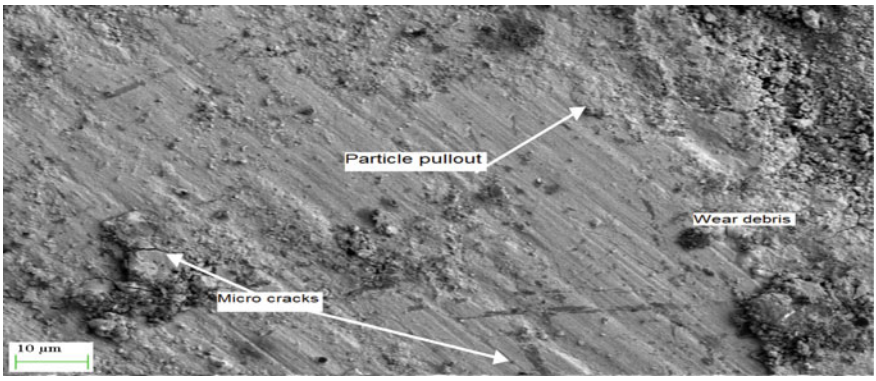

Fig. 15 SEM micrograph of T6-aged Al 6082 alloy with 1 wt % of coarse Al_2O_3 revealing particle pull out, wear debris and micro cracks

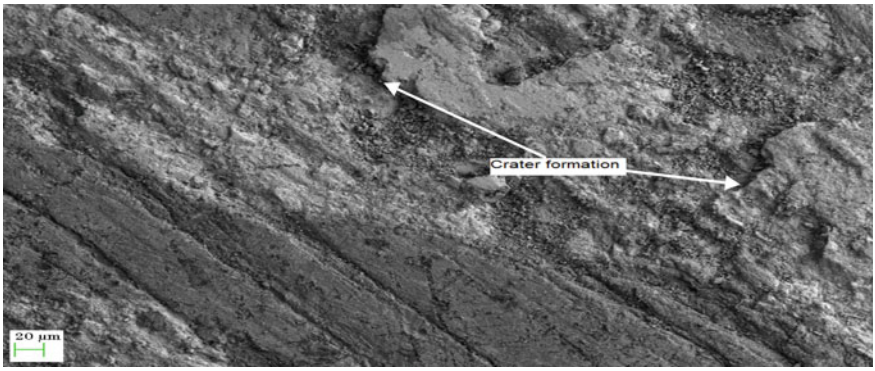

Fig. 16 SEM micrograph of non-aged Al 6082 with 1.5 wt% of coarse Al_2O_3 revealing crater formation due to macroploughing

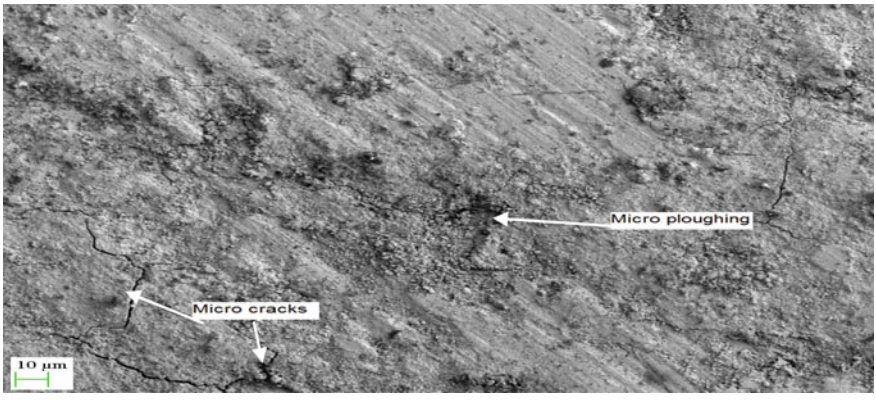

Fig. 17 SEM micrograph of T6-aged Al 6082 alloy with 1.5 wt% of nano Al_2O_3 showing microcracks and microploughing

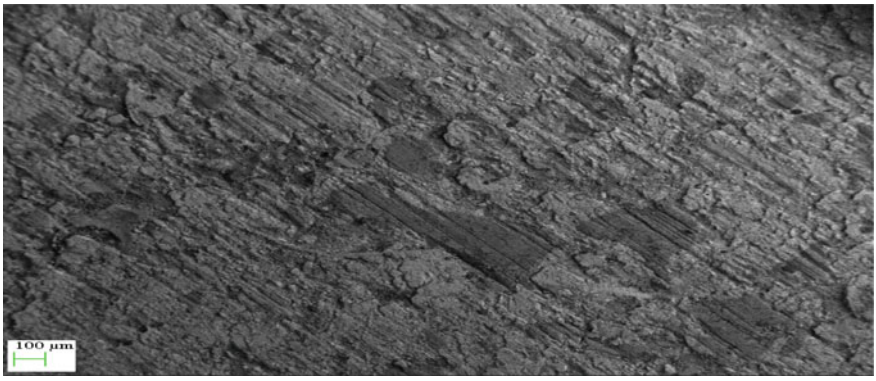

Fig. 18 SEM micrograph of T6-aged Al 6082 with 2 wt% of coarse Al_2O_3 at an applied load of 30 N

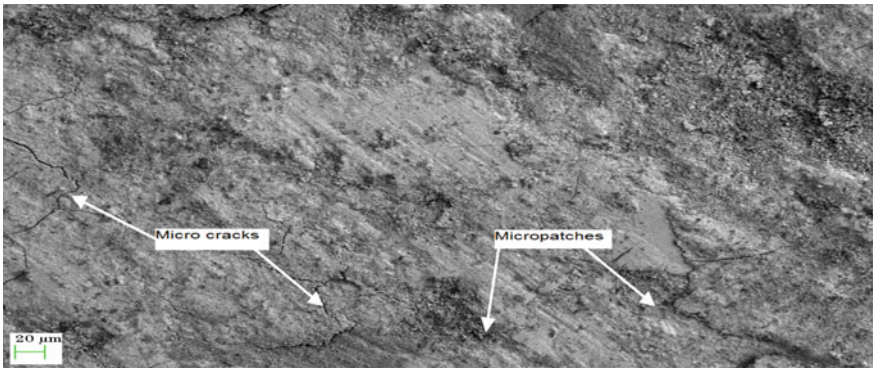

Fig. 19 SEM micrograph of T6-aged Al 6082 alloy with 2 wt% of nano Al_2O_3 revealing micropatches and microcracks due microploughing

shear loads during sliding operation due to which the damage on account of plastic deformation reduces, thus contributing to reduced wear rate of the reinforced and aged specimens. Another contributing factor is the formation of oxide layer on the pin's surface. As the sliding continues, the distortion and fragmentation of the pin mating surface occurs. The displacement of oxides occur with an increase in the applied load; however, a small portion of the oxides between the faying surfaces continues to exist. Dislodging of oxides takes place during the course of sliding; however, a meagre amount of oxides present between the mating surfaces diminishes the metallic contact on account of which the specimens suffer a very reduced wear damage, in other words an increase in wear resistance [37, 38].

The enhancement of wear behaviour of the T6-aged and reinforced specimens can be ascribed to the stable lubricating film, which forms on the surface of the Al 6082

alloy composite. The wear test results showed that not only the addition of nanoparticles but also the heat treatment given to the test specimens play a very significant role in enhancing the wear resistance of the samples. The composite specimens reinforced with nano-Al_2O_3 particles showed an enhanced wear behaviour in terms of reduced volumetric wear loss (refer Figs. 6, 8, 10 and 12). The pin-on-disc tests conducted also indicated that the T6-aged specimens reinforced with nano-Al_2O_3 outperformed the non-aged and coarse Al_2O_3-reinforced samples in terms of increase in wear resistance under varying load conditions. The fragmentation and fracture of the reinforcement media lead to a direct contact between the composite's surface and the counter steel disc. The higher wear resistance of the ceramic-reinforced composite specimens is because of the better load bearing ability of the nano-sized Al_2O_3 reinforcement [37]. The worn surface of the composite specimens shows a mechanically mixed layer deposits as a result of transfer of material from the counter steel disc surface. During pin-on-disc wear testing, the presence of hard ceramic particles acts as stress absorbers during the application of varying applied loads which leads to scratching on the counter steel disc surface.

During sliding operations at varying loads, exposure of the embedded ceramic particles causes localized milling on the counter steel disc surface leading to transfer of steel fragments on the pin's surface. When the composite pin slides against the counter steel disc surface, the disc undergoes severe plastic deformation and leads to the ploughing out of the Iron (Fe) from the rotating counter steel disc surface, which acts as a precursor for the formation of what is known as the mechanically mixed layer (MML). Thus, the test specimen's surface comprises of layers of Fe and FeO which can be confirmed by the EDS analysis as shown in Fig. 20. The decrease in the volumetric wear rate of the reinforced specimens could be attributed to the increase in the weight% of Al_2O_3 particles which reduces the direct contact between the pin's surface and the counter steel disc. When the applied load is less, the effect due to strain hardening is very minimal hence its effect on the wear rate is also very less. Nevertheless, with an increase in the applied load, debonding and fragmentation of ceramic particles from the base matrix occurs. This condition also leads to three-body abrasion. Thus, the increase in wear rate of the samples with an increase in the applied load could be due to the freely moving ceramic particles which act as three-body abrasive elements during pin-on-disc wear testing operations.

At the inception of the pin-on-disc wear testing, the sliding of the pin's surface against the rotating steel disc gradually increases the temperature between the faying surfaces. The effect due to friction between the faying surfaces increases the extent of plastic deformation and hence increases further loss of material. The applied load also has a significant impact on the volumetric wear rate of the composite samples. The rate of wear increases with the increase in the applied load for both unreinforced and reinforced samples. The unreinforced specimens suffer severe damage (plastic deformation) due to direct contact between the pin and counter steel disc surface resulting in a large amount of material removal and subsurface cracking. However, the ceramic particulate-reinforced Al 6082 alloy composite comparatively suffered less damage due to the ability of the Al_2O_3 reinforcement to absorb and withstand the applied load thereby protecting the softer matrix of the base alloy.

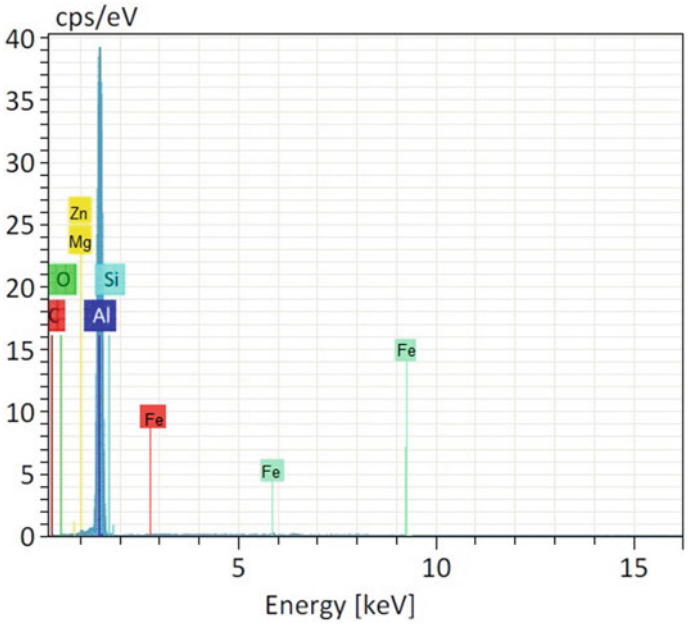

Fig. 20 EDS analysis of T6-aged Al 6082 alloy composite

Thus, the main purpose of the ceramic reinforcement is to reduce surface damage due to plastic deformation and abrasion between the composite pin and steel disc surface thereby reducing the material loss [39, 40].

The addition of reinforcement led to an increase in the dislocation density on account of thermal mismatch between the alloy and the ceramic reinforcement. Due to the presence of large amount of dislocation densities along with the ceramic reinforcement, strain hardening occurs leading to hindrance of dislocation motion contributing to reduced wear rate. With increase in the applied load, a large amount of stress on the contact asperities leads to its fragmentation and particle pull out [40]. The presence of hard asperities in the pin erodes the rotating steel disc surface. Initially, the sharp asperities causes abrasive action on the steel disc causing some portion of the material from the steel disc surface to get transferred to the pin's surface. A previous study [41] demonstrates that the wear resistance of overaged Al-based composites reduces on account of the coarsening of precipitates. On the other hand, the T6 (peak aged) specimens demonstrate an enhanced wear resistance due to the load bearing capacity of the ceramic particulates and the stable Mg_2Si precipitates. The stable Mg_2Si precipitates not only enhanced the bonding between the Al_2O_3 reinforcement and the base matrix but also provided high temperature (thermal) resistance during dry sliding wear tests [40, 43, 43].

Thus, a combination of artificial aging and the addition of increasing weight fraction and decreasing particle size of Al_2O_3 enhanced the hardness and wear resistance of the ceramic-reinforced Al 6082 alloy composite [39–41, 43–47].

4 Conclusions

Al 6082 alloy and Al 6082 alloy composite samples reinforced with varying weight fraction and particle size of alumina particles were synthesized by stir casting process. The solutionized composite specimens were subjected to various durations of heat treatment (i.e., artificial aging) to study its effect on hardness and wear behaviour. XRD analysis confirms the formation of the stable Mg_2Si precipitates. The VHN microhardness results showed that peak aged hardness was attained after 6 h of heat treatment at 180 °C. A maximum peak aged (T6-aged) hardness of 238 VHN was obtained for composite samples reinforced with 2.5% of nano-Al_2O_3. The VHN results demonstrated that the composite samples reinforced with nano-Al_2O_3 particles outperformed the coarse Al_2O_3 reinforced samples with a maximum hardness of 122 VHN after 4 h of aging. Overaging for both sets of samples (coarse and nano-Al_2O_3 reinforced) occurred in the range of 18–20 h. Thus, hardness test showed a better behaviour for alumina added composite due to precipitation hardening. The pin-on-disc wear tests conducted under varying loads, also indicate that the T6-aged samples reinforced with Al_2O_3 particles outperformed the aged as well as non-aged unreinforced Al 6082 alloy samples in terms of reduced volumetric wear rate. Worn surface morphology (FESEM) of the unreinforced sample shows severe damage due to macroploughing revealing poor resistance to wear. The T6-aged samples demonstrated lesser amount of damage compared to the non-aged samples demonstrating enhancement of its hardness and wear resistance. The formation of precipitates which acted as obstacles to dislocation motion during artificial aging acted as stress absorbing elements, resisting the applied loads during dry sliding wear tests. Thus, the present investigation reveals the beneficial influence of both T6 aging as well as the addition of increasing weight fraction and decreasing particle size of Al_2O_3 particles in enhancing the hardness and wear behaviour of Al 6082 alloy.

Acknowledgements The authors would like to acknowledge Dr. N. Srirangarajalu, MIT, Chennai, India, for providing the facilities to do the research work.

References

1. Rahimian M, et al (2009) The effect of particle size, sintering temperature and sintering time on the properties of Al–Al2O3 composites, made by powder metallurgy. J Mater Process Technol 209.14(2009):5387–5393
2. Sharifi EM, Karimzadeh F, Enayati MH (2011) Fabrication and evaluation of mechanical and tribological properties of boron carbide reinforced aluminum matrix nanocomposites. Mater Design 32(6):3263–3271
3. Hemanth J (2009) Quartz (SiO2p) reinforced chilled metal matrix composite (CMMC) for automotive applications. Materials & Design, 30(2), 323-329.
4. Moses JJ, Dinaharan I, Sekhar SJ (2016) Predicting the influence of process parameters on tensile strength of AA6061/TiC aluminum matrix composites produced using stir casting.

5. Zhu QJ, Wang BB, Zhao X, Zhang BB (2018). Robust micro arc oxidation coatings on 6061 aluminum alloys via surface thickening and microvoid reducing approach. In Solid State Phenomena, , Trans Tech Publications Ltd, vol 279, pp. 148–152
6. Dong GJ, Bi J, Du B, Chen XH, Zhao CC (2017) Research on AA6061 tubular components prepared by combined technology of heat treatment and internal high pressure forming. J Mater Process Technol 242:126–138
7. Yu LI, Li QL, Dong LI, Wei LIU, Shu GG (2016) Fabrication and characterization of stir casting AA6061—31% B4C composite. Trans Nonferrous Metal Soc China 26(9):2304–2312
8. Kang YC, Chan SLI (2004) Tensile properties of nanometric Al2O3 particulate-reinforced aluminum matrix composites. Mater Chem Phys 85(2–3):438–443
9. Namini AS, Azadbeh M, Asl MS (2017) Effect of TiB2 content on the characteristics of spark plasma sintered Ti–TiBw composites. Adv Powder Technol 28(6):1564–1572
10. Sharma, P., Khanduja, D., & Sharma, S. (2014). Metallurgical and Mechanical characterization of Al 6082-B4C/Si3N4 hybrid composite manufactured by combined ball milling and stir casting. In Applied Mechanics and Materials (Vol. 592, pp. 484-488). Trans Tech Publications Ltd.
11. El-Danaf EA, El-Rayes MM (2013) Microstructure and mechanical properties of friction stir welded 6082 AA in as welded and post weld heat treated conditions. Mater Design 46:561–572
12. Thangarasu A, Murugan N, Mohankumar R, Thangapandi P (2014) Processing and characterization of AA6082/TiC composites by stir casting. Emer Mater Res 3(3):123–129
13. Ravi KR, Sreekumar VM, Pillai RM, Mahato C, Amaranathan KR, Pai BC (2007) Optimization of mixing parameters through a water model for metal matrix composites synthesis. Mater Design 28(3):871–881
14. Kok M (2005) Production and mechanical properties of Al2O3 particle-reinforced 2024 aluminium alloy composites. J Mater Process Technol 161(3):381–387.
15. Mazahery, A., & Shabani, M. O. (2012). Tribological behaviour of semisolid–semisolid compocast Al–Si matrix composites reinforced with TiB2 coated B4C particulates. Ceram Int 38(3):1887–1895
16. Suresh S, Moorthi NSV, Vettivel SC, Selvakumar N (2014) Mechanical behavior and wear prediction of stir cast Al–TiB^2 composites using response surface methodology. Mater Design 59:383–396
17. Razavizadeh K, Eyre TS (1982) Oxidative wear of aluminium alloys. Wear 79(3):325–333
18. Lai J, Zhang Z, Chen XG (2013) Precipitation strengthening of Al–B^4C metal matrix composites alloyed with Sc and Zr. J Alloy Comp 552:227–235
19. Bueno S, Ferrari B, Melandri C, De Portu G, Baudín C (2010) Processing of alumina-coated tetragonal zirconia materials and their response to sliding wear. Ceram Int 36(5):1545–1552
20. Su H, Gao W, Feng Z, Lu Z (2012) Processing microstructure and tensile properties of nano-sized Al2O3 particle reinforced aluminum matrix composites. Mater Design (1980–2015), 36:590–596
21. Zhang Q, Ma X, Wu G (2013) Interfacial microstructure of SiCp/Al composite produced by the pressureless infiltration technique. Ceram Int 39(5):4893–4897
22. El-Sabbagh AM, Soliman M, Taha MA, Palkowski H (2013) Effect of rolling and heat treatment on tensile behaviour of wrought Al-SiCp composites prepared by stir-casting. J Mater Process Technol 213(10):1669–1681
23. Mohamed MS, Foster AD, Lin J, Balint DS, Dean TA (2012) Investigation of deformation and failure features in hot stamping of AA6082: experimentation and modelling. Int J Mach Tool Manuf 53(1):27–38
24. Shaeri MH, Salehi MT, Seyyedein SH, Abutalebi MR, Park JK (2014) Microstructure and mechanical properties of Al-7075 alloy processed by equal channel angular pressing combined with aging treatment. Mater Design 57:250–257
25. Cong FG, Gang ZHAO, Jiang F, Ni TIAN, Li RF (2015) Effect of homogenization treatment on microstructure and mechanical properties of DC cast 7X50 aluminum alloy. Trans Nonferrous Metals Soc China 25(4):1027–1034

26. Kök M, Özdin K (2007) Wear resistance of aluminium alloy and its composites reinforced by Al^2O^3 particles. J Mater Process Technol 183(2–3):301–309
27. Surappa MK, Prasad, SV, Rohatgi PK (1982) Wear and abrasion of cast Al-alumina particle composites. Wear, 77(3):295–302
28. Appendino P, Badini C, Marino F, Tomasi, A (1991) 6061 aluminium alloy-SiC particulate composite: a comparison between aging behavior in T4 and T6 treatments. Mater Sci Eng A 135:275–279
29. Kumar, G. V., Pramod, R., Gouda, P. S., & Rao, C. S. P. (2018). Effect of tungsten carbide reinforcement on the aluminum 6061 alloy. J Test Evaluat 47(4):2613–2629
30. Ramesh CS, Safiulla M (2007) Wear behavior of hot extruded Al6061 based composites. Wear 263(1–6):629–635.
31. Chawla KK, Esmaeili AH, Datye AK, Vasudevan AK (1991) Effect of homogeneous/heterogeneous precipitation on aging behavior of SiCPAl 2014 composite. Scripta Metallurgica et Materialia, 25(6):1315–1319
32. Yılmaz O, Buytoz S (2001) Abrasive wear of Al2O3-reinforced aluminium-based MMCs. Compos Sci Technol 61(16):2381–2392
33. Kaushik NC, Rao RN (2016) Effect of grit size on two body abrasive wear of Al 6082 hybrid composites produced by stir casting method. Tribol Int 102:52–60
34. Kaushik NC, Rao RN (2016) Effect of applied load and grit size on wear coefficients of Al 6082–SiC–Gr hybrid composites under two body abrasion. Tribol Int 103:298–308
35. Salvo L, L'esperance G, Suery M, Legoux JG (1994) Interfacial reactions and age hardening in Al Mg Si metal matrix composites reinforced with SiC particles. Mater Sci Eng: A 177(1–2):173–183
36. Udayashankar, N. K., Rajasekaran, S., & Nayak, J. (2012). The effect of protective coatings on the oxidation behavior of 6061Al/SiC composite at high temperatures. In Advanced Materials Research, Trans Tech Publications Ltd. vol 383, pp 3949–3953
37. Savaşkan T, Hekimoğlu AP, Pürçek G (2004) Effect of copper content on the mechanical and sliding wear properties of monotectoid-based zinc-aluminium-copper alloys. Tribol Int 37(1):45–50
38. Prasad Reddy A, Vamsi Krishna P, Rao RN (2019) Two-body abrasive wear behaviour of AA6061-2SiC-2Gr hybrid nanocomposite fabricated through ultrasonically assisted stir casting. J Compos Mater 53(15):2165–2180
39. Mazahery A, & Shabani MO (2013) Microstructural and abrasive wear properties of SiC reinforced aluminum-based composite produced by compocasting. Trans Nonferrous Metal Soc China 23(7):1905–1914
40. Gurcan AB, Baker TN (1995) Wear behaviour of AA6061 aluminium alloy and its composites. Wear 188(1–2): 185–191
41. Gavgali M, Totik Y, Sadeler R (2003) The effects of artificial aging on wear properties of AA 6063 alloy. Mater Let 57(24–25): 3713–3721
43. Song WQ, Krauklis P, Mouritz AP, Bandyopadhyay S (1995) The effect of thermal ageing on the abrasive wear behaviour of age-hardening 2014 Al/SiC and 6061 Al/SiC composites. Wear 185(1–2):125–130
44. Das S, Mondal DP, Sawla S, Ramakrishnan N (2008) Synergic effect of reinforcement and heat treatment on the two body abrasive wear of an Al–Si alloy under varying loads and abrasive sizes. Wear 264(1–2):47–59
45. Dasgupta R (2010) Sliding wear resistance of Al-alloy particulate composites: An assessment on its efficacy. Tribol Int 43(5–6):951–958
46. Alaneme KK, Adegun MH, Archibong AG, Okotete EA (2019) Mechanical and wear behaviour of aluminium hybrid composites reinforced with varied aggregates of alumina and quarry dust. J Chem Technol Metallurgy 54(6)
47. Bonny K, De Baets P, Vleugels J, Van der Biest O, Salehi A, Liu W, Lauwers B (2009) Reciprocating sliding friction and wear behavior of electrical discharge machined zirconia-based composites against WC–Co cemented carbide. Int J Refract Metals Hard Mater 27(2):449–457